Tactile Exploration Using Unified Force-Impedance Control

Kübra Karacan, Divij Grover, Hamid Sadeghian, Fan Wu, and Sami Haddadin

The Chair of Robotics and Systems Intelligence, MIRMI - Munich Institute of Robotics and Machine Intelligence, Technical University of Munich, Germany, Centre for Tactile Internet with Human-in-the-Loop (CeTI). H. Sadeghian also has an affiliation with University of Isfahan.

Abstract: Tactile robots can perform complex interaction skills, e.g., polishing. Such robots should therefore be designed to be adaptive to environmental uncertainties such as changing geometry and contact-loss. To address this, we propose a tactile exploration technique to observe the local curvatures of the physical constraints such as corners, edges, etc. for updating predefined tactile skill policies accordingly. First, we develop a unified force-impedance control approach in which the force controller significantly improves the geometry following performance due to the ensured contact. Second, we use the proposed controller to autonomously investigate the unknown environment via the local curvature observer, designed to be a dynamic process. Finally, the exploration performance of the proposed controller is demonstrated by using a polishing skill on an unknown 3D surface, where the robot is observed to autonomously investigate the unknown surface from top to bottom along the edges and corners.

Keywords: Intelligent robotics, Autonomous robotic systems

1. INTRODUCTION

Robotic systems have been deployed in human sectors such as manufacturing, production, and service since the introduction of industrial robots. Such human sectors involve complex interaction tasks that must be executed in dynamic and unstructured environments. Traditional position-controlled industrial robots lack these adaptable and versatile characteristics. While new generation torque-controlled robots, as discussed by Hirzinger et al. (2001), provide the option of compliant behaviors via admittance control in Shahriari et al. (2017), impedance control in Hogan (1984), or force control in Khatib (1987). Additionally, Kirschner et al. (2021) demonstrated that the type of robot and controller are key factors in interaction skill performance.

Haddadin et al. (2019) discusses extensively the key to the use of tactile robots for performing complex interaction skills such as polishing is to utilize their ability of the recognition of touch. Preferably, as argued by Karacan et al. (2022), the human operator should give the archetypical solution to such robots, along with the desired tactile actions such as force and motion policies. Using polishing as an example, the human operator instructs the robot to polish a scratch on a surface with a desired force. However, the robot should be programmed to be adaptive to environmental uncertainties such as contact loss, which can damage the robot or the surrounding environment during applying force.

The state-of-the-art in tactile robot programming, on the other hand, still demands a fairly accurate model of the environment. Furthermore, not only is the task becoming more complex, but transferring it to a different environment demands re-programming and, as a result, expert knowledge, as shown in Johannsmeier et al. (2019). Hence, new solutions to ease the (re-)programming of tactile tasks must be developed for increased flexibility and adaptation in tactile robot capabilities, see the study of Haddadin et al. (2022). To address the aforementioned problems, tactile exploration is a useful approach to

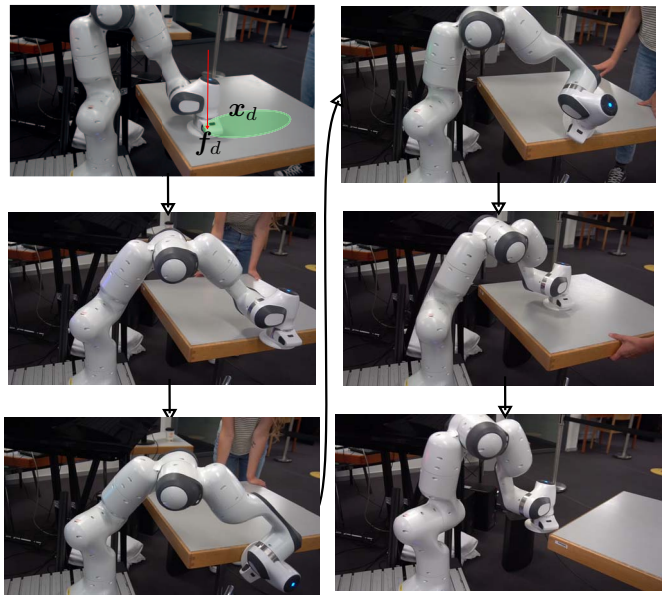

Fig. 1. Tactile exploration via local curvature observer. The robot follows a desired Cartesian motion while constantly applying a desired force in the z-direction. When the robot encounters an edge of the table (a 90-degree cliff), it rotates and adapts itself. If the contact is completely lost, the robot stops the force controller.

⋆ Corresponding Author: Kübra Karacan kuebra.karacan@tum.de

investigate the unknown environment. Haddadin et al. (2010) and Haddadin et al. (2011) previously studied tactile exploration by leveraging novel collision avoidance algorithms and achieved preliminary results.

In this work, we develop an advanced tactile exploration strategy based on unified force-impedance control. Our novel exploration strategy investigates unknown environments via local curvature observer in real-time manner, designed to be a dynamic process (see Fig. 1). First, we develop a unified force-impedance control approach that allows the robot to adjust its impedance parameters to the environment. Here, the force controller is crucial as it significantly increases the geometry following performance due to the ensured contact. Second, we use the proposed controller to investigate autonomously the environment by observing the local curvatures. Finally, the tactile exploration performance of the controller is proven by using a polishing skill on an unknown 3D surfaces. The proposed method is used to polish a table from the top surface to its edges and finally to the bottom surface without knowing the model of the environment.

The rest of the paper is presented as follows. Section 2 discusses the related literature, and Sec. 3 introduces our novel unified force-impedance control-based tactile exploration strategy and the local curvature observer for tactile skills. The experimental protocol and the corresponding results are demonstrated in Sec. 4 and Sec. 5. Lastly, Sec. 6 finalizes the paper.

2. RELATED LITERATURE

Robotic tactile skills such as polishing, filing, and grinding need accurate control of interaction to the end-effector. Namely, force and motion policies should be combined to develop tactile skills. Hence, robotic systems need to develop complex perceptuo-motor abilities to handle such skills, as studied in Pastor et al. (2011). Furthermore, Hogan (1984) shows that position control is insufficient to realize such tactile skills and alternative control strategies should be considered, such as e.g., force control in Khatib (1987), using admittance control in Shahriari et al. (2017), and even unified methods in Schindlbeck and Haddadin (2015).

Additionally, numerous works have taken into account force control, validating the suggested controllers using constant force values or as thresholds or limitations, as discussed in Ficuciello et al. (2015); Kulakov et al. (2015); Ott et al. (2015); He et al. (2016). The robots must, however, be smart enough to operate autonomously in uncertain environments and complete required tasks when faced with perception uncertainties, shown in Pastor et al. (2012); Kramberger et al. (2016).

To attain a more human-like response for the contact at the end-effector, adaptive adjustment of the impedance parameters is helpful in many applications such as Yang et al. (2011). The Wavelet Neural Network has been applied by Hamedani et al. (2021) to integrate compliant force tracking on the unknown geometry.

Force information and historical position from the end-effector is used to predict shape profile in Qian et al. (2019). In another study, Lepora and Lloyd (2020) developed new tactile capabilities with the soft tactile sensors and neural networks include using a pose-based servo control, where a tactile fingertip mounted on a robot arm slides delicately over unknown complex 3D objects. There exist other exploration approaches such as using mechanics in Balatti et al. (2020), learning (offline) in Simonič et al. (2019), and control theory in Kato et al. (2022).

In this paper, we propose a unified force-impedance control-based tactile exploration technique to observe the local curvatures of the physical constraints to understand corners, edges, etc., for updating the predefined tactile skill policies accordingly. First, we develop a unified force-impedance control approach that allows the robot to adjust its impedance parameters to the unknown environment. Using force control, in particular, makes exploration easier as the contact is ensured during the process. Second, we propose a dynamic process to observe the local curvature of the environment, and use it to align the tool while exploring the corresponding contact surface. Finally, the exploration performance of the controller is demonstrated by using a polishing skill on an unknown 3D surfaces.

3. METHODOLOGY

A robot expert establishes a tactile skill library relying on intuitive estimation of the physical constraints of the environment. Using the polishing skill as an instance, the robot expert trains the robot with certain tactile action policies, including the motion and force profiles. Yet, carrying out of the desired task, the robot should have the autonomy to adjust those intended tactile action policies to the entirely or partially unknown environment. Even if the robot has an external sensing capability, such as a camera, it may still operate within tolerance, particularly under a fairly cluttered environment. Hence, the tactile skills should be developed to allow the robot to adjust the appropriate tactile skills to the surroundings with as little interference from outside as possible.

Considering the fact that the robot runs a tactile skill defined for certain conditions, changes in the geometry could be inferred from the local curvature. Here, we use an exploration strategy to investigate the physical constraints of the environment such as corners and edges via local curvature observer. The exploration strategy utilizes adaptive-stiffness of the impedance controller as well as the robust contact via force controller, see Fig.2. Additionally, the recorded geometry information of the physical constraint might further be used to generate motion and force profiles for a new surface.

3.1 Preliminaries

The dynamics equation for a robot with n-DOF in Cartesian space is

$$\boldsymbol{M}_C(\boldsymbol{q})\ddot{\boldsymbol{x}} + \boldsymbol{C}_C(\boldsymbol{q},\dot{\boldsymbol{q}})\dot{\boldsymbol{x}} + \boldsymbol{f}_g(\boldsymbol{q}) = \boldsymbol{f}_{\text{in}} + \boldsymbol{f}_{\text{ext}}\,, \qquad (1)$$

where $\boldsymbol{x}$, $\dot{\boldsymbol{x}} \in \mathbb{R}^6$ are the Cartesian pose and twist. The external wrench on the robot is $\boldsymbol{f}_{\text{ext}} \in \mathbb{R}^6$. $\boldsymbol{M}_C(\boldsymbol{q})$, $\boldsymbol{C}_C(\boldsymbol{q},\dot{\boldsymbol{q}}) \in \mathbb{R}^{6\times 6}$, and $\boldsymbol{f}_g(\boldsymbol{q})$ are the robot mass matrix, the Coriolis and centrifugal matrix, and the gravity vector in Cartesian space, respectively. Additionally, $\boldsymbol{f}_{\text{in}}$ is the input wrench in Cartesian space and relates to the joint torques via robot's Jacobian matrix $\boldsymbol{J} \in \mathbb{R}^{6\times n}$ $\boldsymbol{\tau}_{\text{in}} \in \mathbb{R}^n$ by $\boldsymbol{\tau}_{\text{in}} = \boldsymbol{J}^T(\boldsymbol{q})\boldsymbol{f}_{\text{in}}$.

3.2 Controller Design

The proposed control law for exploration is extended from unified force-impedance control by Schindlbeck and Haddadin (2015) with four main components:

I) tracking the desired Cartesian pose $\boldsymbol{x}_d$ with the impedance controller,

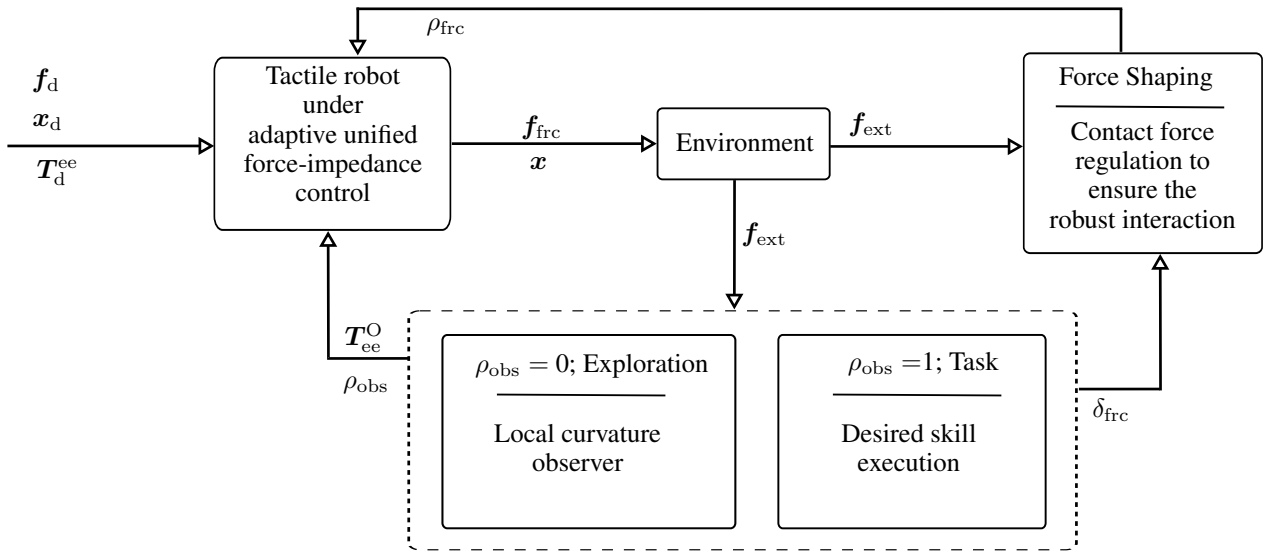

Fig. 2. Block diagram for unified force-impedance control-based local curvature observer for tactile exploration architecture. The predefined tactile skills are adjusted to the unknown environment by using force shaping ρ_{frc} and exploration blocks. The state switching is handled via ρ_{obs}.

II) exploring the transformation matrix $\boldsymbol{T}_{\text{ee}}^{0}$,
III) following the commanded force $\boldsymbol{f}_d$, and
IV) gravity compensation $\boldsymbol{\tau}_g$.

The input torque $\boldsymbol{\tau}_{\text{in}} \in \mathbb{R}^n$ is:

$$\boldsymbol{\tau}_{\text{in}} = \boldsymbol{\tau}_{\text{imp}} + \boldsymbol{\tau}_{\text{frc}} + \boldsymbol{\tau}_g \,, \tag{2}$$

where $\boldsymbol{\tau}_{\text{imp}}$, $\boldsymbol{\tau}_{\text{frc}}$, and $\boldsymbol{\tau}_g \in \mathbb{R}^n$ are the input torques with respect to (i) impedance control (ii) force control and (iii) gravity compensation.

Impedance Control In order to establish a desired Cartesian impedance behavior at the tool, the following control law is defined

$$\begin{aligned} \boldsymbol{\tau}_{\text{imp}} &= \boldsymbol{J}^T(\boldsymbol{q})(\boldsymbol{K}_C\tilde{\boldsymbol{x}} + \boldsymbol{D}_C\dot{\tilde{\boldsymbol{x}}} + \boldsymbol{M}_C(\boldsymbol{q})\ddot{\boldsymbol{x}}_d + \boldsymbol{C}_C(\boldsymbol{q},\dot{\boldsymbol{q}})\dot{\boldsymbol{x}}_d), \\ \tilde{\boldsymbol{x}} &= \boldsymbol{x}_d - \boldsymbol{x}, \end{aligned} \tag{3}$$

where $\boldsymbol{x} \in \mathbb{R}^6$ is the actual pose and the pose error is $\tilde{\boldsymbol{x}}$. Moreover, $\boldsymbol{K}_C, \boldsymbol{D}_C \in \mathbb{R}^{6\times6}$ are time-varying stiffness and damping matrices, respectively. The desired Cartesian inertia is assumed to be the actual robot inertia in Cartesian space.

Force Control To control the desired force at the end effector $\boldsymbol{f}_{\text{d}}^{\text{ee}} \in \mathbb{R}^6$ w.r.t the external force $\boldsymbol{f}_{\text{ext}}^{\text{ee}} \in \mathbb{R}^6$, we design the controller as follows,

$$\boldsymbol{\tau}_{\text{frc}} = \rho_{\text{frc}}\boldsymbol{J}(\boldsymbol{q})^T \begin{bmatrix} [\boldsymbol{R}_{\text{ee}}^{\text{O}}]_{3\times3} & \boldsymbol{0}_{3\times3} \\ \boldsymbol{0}_{3\times3} & [\boldsymbol{R}_{\text{ee}}^{\text{O}}]_{3\times3} \end{bmatrix} \boldsymbol{f}_{\text{frc}}^{\text{ee}}, \tag{4}$$

$$\boldsymbol{f}_{\text{frc}}^{\text{ee}} = \boldsymbol{f}_d^{\text{ee}} + \boldsymbol{K}_p\,\tilde{\boldsymbol{f}}_{\text{ext}}^{\text{ee}} + \boldsymbol{K}_i \int \tilde{\boldsymbol{f}}_{\text{ext}}^{\text{ee}}\, dt + \boldsymbol{K}_d\,\dot{\tilde{\boldsymbol{f}}}_{\text{ext}}^{\text{ee}}\,, \tag{5}$$

$$\tilde{\boldsymbol{f}}_{\text{ext}}^{\text{ee}} = \boldsymbol{f}_d^{\text{ee}} + \boldsymbol{f}_{\text{ext}}^{\text{ee}}, \tag{6}$$

where $\boldsymbol{f}_{\text{frc}}^{\text{ee}} \in \mathbb{R}^6$ is a feedback force controller output with the diagonal matrices of the PID gains $\boldsymbol{K}_p, \boldsymbol{K}_i, \boldsymbol{K}_d \in \mathbb{R}^{6\times6}$. Furthermore, force shaping function ρ_{frc} decides to activate or deactivate the force controller based on certain conditions.

Force Shaping Function In unified force-impedance control, if the pose error in any direction is beyond the predefined threshold for a direction δ_{frc}, for example, due to the environment change, the shaping function presents the contact-loss behavior and starts the force shaping function ρ_{frc}, which degrades the effect of the force controller. In order to ensure a smooth transition, instead of a chattering behavior, ρ_{frc} interpolates in a user defined threshold δ_{frc}. δ_{frc} is the distance range in which the robot can move safely after the contact-loss takes place, while still exerting some force in the desired direction. The magnitude of force is however regulated by the force shaping function ρ_{frc}. Increasing δ_{frc} also increases the range of motion in which the robot is allowed to move while keep applying the force in the desired direction. Consequently, ρ_{frc} is

$$\rho_{\text{frc}} = \begin{cases} 1\,, & \boldsymbol{f}_d^{\text{ee}T}\tilde{\boldsymbol{x}}^{\boldsymbol{ee}} \geq 0 \\ 0.5(1+\cos(\pi(\frac{|\tilde{x}_z^{ee}|}{\delta_{\text{frc}}}))\,, & \boldsymbol{f}_d^{\text{ee}T}\tilde{\boldsymbol{x}}^{\boldsymbol{ee}} < 0 \\ & \wedge\, 0 < |\tilde{x}_z^{ee}| \leq \delta_{\text{frc}} \\ 0\,, & \text{else} \end{cases} \tag{7}$$

Finally, the closed loop equation for the overall system becomes

$$\boldsymbol{M}_C(\boldsymbol{q})\ddot{\tilde{\boldsymbol{x}}} + \boldsymbol{C}_C(\boldsymbol{q},\dot{\boldsymbol{q}})\dot{\tilde{\boldsymbol{x}}} + \boldsymbol{D}_C\dot{\tilde{\boldsymbol{x}}} + \boldsymbol{K}_C\tilde{\boldsymbol{x}} + \boldsymbol{f}_{\text{frc}} + \boldsymbol{f}_{\text{ext}} = 0\,. \tag{8}$$

3.3 Tactile Exploration Strategy

The state machine in Fig. 3 explains the exploration strategy. Exploration consists of three major states: adaptation, task, and contact-loss. State adaptation allows the end-effector to adjust itself to the physical constraints of the environment.

The end effector of the robot is equipped with a tool with certain dimensions. When the tool is at an angle with the surface, the external force in z direction $\boldsymbol{f}_{\text{z}}^{\text{ee}}$ creates a moment about x and y-axis $\boldsymbol{M}_{\text{xy,ee}} = [\boldsymbol{M}_{\text{x,ee}}\ \boldsymbol{M}_{\text{y,ee}}] \in \mathbb{R}^2$. L_2 norm of moments about x and y-axis $\|\boldsymbol{M}_{\text{xy,ee}}\|_2$ gives us the length of $\boldsymbol{M}_{\text{xy,ee}}$. Thus, local curvature *lc* is given as fraction of $\boldsymbol{M}_{\text{xy,ee}}$ and $\boldsymbol{f}_{\text{z}}^{\text{ee}}$. *lc* greater than the threshold value indicates that the tools need to be realigned to the surface.

Here, the curvature observer ρ_{obs} is computed from a normalized curvature coefficient α

$$\alpha = \frac{lc_{\text{threshold}} - lc}{lc_{\text{threshold}}}\,, \tag{9}$$

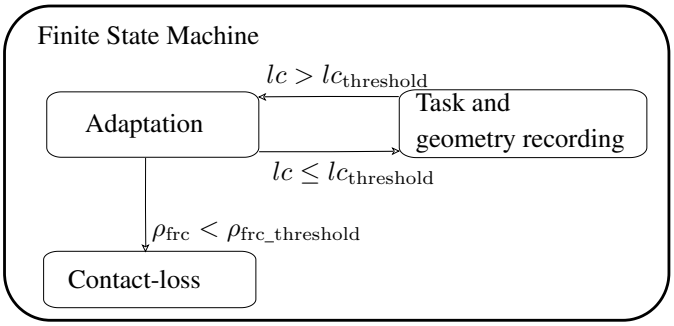

Fig. 3. State machine for exploration in simplified form. When the robot is in exploration state, the rotational stiffness about x- and y- directions $\boldsymbol{K}_{r,x}$ and $\boldsymbol{K}_{r,y}$ is zero. This allows the robot to follow the unknown geometry while it moves via the translational stiffness. And the stiffness matrix of the end-effector is also rotated.

where the curvature observer ρ_{obs} is obtained by the dynamics

$$\dot{\rho}_{\text{obs}} = \begin{cases} \min\{\rho, 0\}\,, & \rho_{\text{obs}} = 1 \\ \rho\,, & 0 < \rho_{\text{obs}} < 1,\ \rho_{\text{obs}}(0) = 0, \\ \max\{\rho, 0\}\,, & \rho_{\text{obs}} = 0 \end{cases} \tag{10}$$

and ρ is given by

$$\rho = \alpha\rho_{\text{obs}} + \rho_{min}. \tag{11}$$

Note that, in order to have an initial increment for the case $\rho_{\text{obs}} = 0$, a small positive constant ρ_{min} has been introduced into the curvature observer dynamics. It is noteworthy that the solution for the curvature observer dynamics allows us to have the behavior for increasing or decreasing exponential function based on the local curvature and, thus, is used to switch the between the exploration motion and the task.

The task state computes the new trajectory $\boldsymbol{T}^0_{\text{ee,traj}}$ to follow, once the contact is re-established. And the robot runs the new trajectory until the end effector is no longer in contact with the environment, i.e., $lc > lc_{\text{threshold}}$ meaning $\rho_{\text{obs}} < 1$. In detailed, *lc* created due to external force $\boldsymbol{f}_{\text{z}}$ on the end effector indicates if the robot is in complete contact with the surface or not, and therefore is included in the curvature observer dynamics as a transition parameter between different states (ρ_{obs} =1 or 0).

Algorithm 1 State adaptation and local curvature observer

Input $M_{x,ee},\ M_{y,ee},\ f_z,\ T^0_{ee}$
Output T^0_d

Initialization: $\{\text{p}^0_{\text{traj}}, \text{R}^0_{\text{traj}}\} = \text{T}^0_{\text{traj}}$,
loop:
$M_{\text{xy,ee}} = ||[M_{\text{x,ee}} M_{\text{y,ee}}]||_2$.
$lc = \frac{M_{\text{xy,ee}}}{f_z}$.
if $\rho_{\text{obs}} < 1$ **then**
    $R^0_{\text{d}} = R^0_{\text{ee}}$
    $p^0_{\text{d}} = p^0_{\text{traj}}$
    $T^0_{\text{d}} = \{p^0_{\text{traj}}, R^0_{\text{ee}}\}$
    $\delta_{\text{frc}} \leftarrow \delta_{\text{frc}} + \delta_{\text{increment}}$
end if
goto *loop*.
close;

The state of contact-loss makes sure that no unwanted rapid motions occur. If $\rho_{\text{frc}} < \rho_{\text{frc,threshold}}$, the contact-loss state stops the robot and prevents unwanted rapid motion that could endanger the robot and the environment.

State adaptation explained in Alg. 1 tries to minimize the moment about x and y-axis. This is done by setting zero rotational stiffness about x and y-axis and at the same time maintaining the last position where the tool unaligned itself. The zero stiffness is achieved by setting the desired orientation around x- and y-axis as current orientation. This can be seen in line 7,8 and 9 in algorithm state adaptation. Therefore, the tool is free to move along x- and y-axis while applying force in desired direction. Moreover, in line 10, the translational distance range δ_{frc} is incremented by the factor of $\delta_{\text{increment}}$ until the end-effector is able to apply the desired force onto the surface. Furthermore, if the tool attached to the end-effector is not in the desired contact with the surface, the reaction force applied by the environment creates a moment about x and y-axis. The resulting moment due to increase in δ_{frc}, zero rotational stiffness about x- and y-axis and low stiffness in z direction causes the robot to move in z-direction and at the same time adapt itself to always stay normal to the surface until the end-effector is able to make complete contact with the surface.

Algorithm 2 State Task and Information Saving

Input $M_{x,ee},\ M_{y,ee},\ f_z,\ T^0_{ee}$
Output T^0_d

Initialization: $\text{T}^0_{\text{ee,temp}} = \text{T}^0_{\text{ee}}$,
loop:
$lc = \frac{M_{\text{xy,ee}}}{f_z}$.
if $\rho_{\text{obs}} = 1$ **then**
    $T^0_{\text{ee,traj}} = T^0_{\text{ee,temp}} T^{\text{ee}}_{\text{d}}$
    $T^0_{\text{d}} = T^0_{\text{ee,traj}}$
    $T^0_{\text{record}} = T^0_{\text{d}}$
end if
goto *loop*.
close;

State task and information saving in Alg. 2 plans the trajectory and saves the current position and orientation of the end effector. This state is only active when the tool is completely aligned with the surface. The $\text{T}^0_{\text{ee,temp}}$ is updated only once at the entry of this state. Finally, the saved data may be used for future motion and force profile generation.

4. EXPERIMENTAL SETUP

To evaluate the exploration, adaptation, and control performance of our framework for the tactile skills to run under unknown physical constraints, the experiments are conducted using a Franka Emika robot for a polishing skill. Polishing requires the robot applying a desired wrench $\boldsymbol{f}^{\text{ee}}_d$ on the surface while tracking a circular motion $\boldsymbol{T}^{\text{ee}}_{\text{d}}(t)$ represented by $\boldsymbol{R} = \boldsymbol{I}_{3\times3}$ and

$$\boldsymbol{p}^{\text{ee}}_{\text{d}}(t) = [0.1\sin(0.5t), 0.1\cos(0.5t), 0]^T\,, \tag{12}$$

$$\boldsymbol{f}^{\text{ee}}_d = [0, 0, 35\,\text{N}, 0, 0, 0]^T\,. \tag{13}$$

The radius of the tool is 0.06 m and therefore the threshold value $\text{lc}_{\text{threshold}}$ is taken as 0.025 m (see Table 1 for other parameters used).

The robot follows a trajectory in one direction while constantly maintaining force in the z-direction. The end-effector is able

Table 1. Parameters used throughout the experiments.

Property	Unit	Value
$\boldsymbol{K}_{\mathrm{c}}$	N/m	diag[1000,1000,10,0,0,70]
$\boldsymbol{\xi}$	Ns/m	diag[0.7,0.7,0.7,1,1,1]
$\mathrm{lc}_{\mathrm{threshold}}$	m	0.025
$\boldsymbol{K}_p, \boldsymbol{K}_i, \boldsymbol{K}_d$	-	$0.5\boldsymbol{I}_{6\times6}, 0.5\boldsymbol{I}_{6\times6}, 0\boldsymbol{I}_{6\times6}$
$\boldsymbol{\delta}_{\mathrm{frc}}(0)$	m	[0.05, 0.05, 0.05, 0.05, 0.05, 0.05]
$\rho_{\mathrm{frc,threshold}}$	-	0.1
ρ_{min}	-	0.001

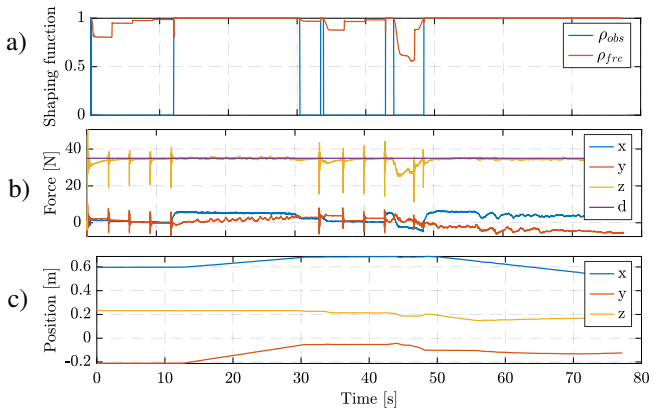

Fig. 4. Experimental results for polishing the car-door. During the contact, ρ_{frc} is 1 and regulates the external force. ρ_{obs} decides the state of the robot (exploration or task) to adapt to the changing geometry. a) Shaping functions ρ_{obs} and ρ_{frc}, b) External force at the end-effector, c) Actual position x, y, and z w.r.t to the robot base frame.

to maintain the full contact, and it moves until the environment changes. In the first set of experiments, the robot should polish a car-door without knowing the geometry of the environment. The expected behavior of the robot is that the end-effector should follow the geometry while polishing it. Second, the robot should polish a table without geometry information. Moreover, when the robot encounters an edge of the table (a 90-degree cliff), it should be able to rotate and adapt itself. The goal is to make sure that the end-effector is always in full contact and aligned with the surface. Additionally, during the experiments, the robot's own internal sensing capabilities are used to obtain the external force/torque measurements, as analyzed by Haddadin et al. (2017).

5. RESULTS AND DISCUSSION

It can be seen in Fig. 4 and Fig. 5 that when the polishing tool is not in complete contact with the environment or the robot starts encountering the cliff, ρ_{frc} starts declining and lc starts increasing (ρ_{obs} decreases to zero), indicating that the tool needs to be realigned to the surface. Thus, the state is switched from the desired task ($\rho_{\mathrm{obs}} = 1$) to tactile exploration ($\rho_{\mathrm{obs}} = 0$). The exploration state is maintained until the polishing tool is completely aligned to the surface, meaning $lc \leq lc_{\mathrm{threshold}}$ and $\rho_{\mathrm{obs}} = 1$. After the polishing tool is adapted to the surface

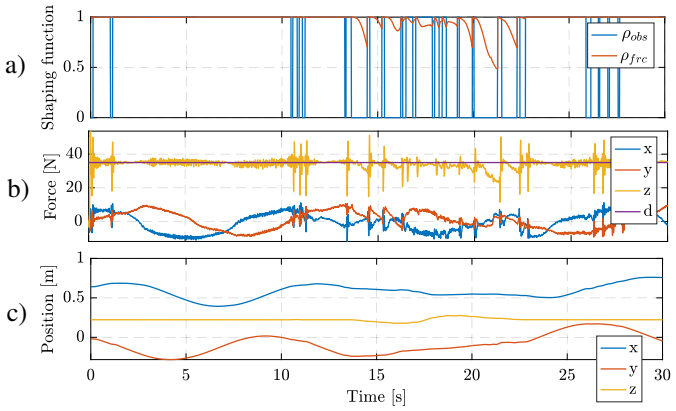

Fig. 5. Experimental results for polishing the table. During the contact, ρ_{frc} is 1 and regulates the external force. ρ_{obs} decides the state of the robot (exploration or task) to adapt to the changing geometry. a) Shaping functions ρ_{obs} and ρ_{frc}, b) External force at the end-effector, c) Actual position x, y, and z w.r.t to the robot base frame.

geometry, the state changes back to the task and the polishing tool starts moving in the desired trajectory again.

It is noteworthy that, the limitation of this approach is that the local curvature observer depends on the type of the desired contact. For instance, the single point contact is unlikely to be achieved by using our method. Additionally, even though the robot adapts the parameters of impedance and force control according to the abrupt changes in the environment, the controller's stability still might be compromised, as discussed by Kronander and Billard (2016). Thus, one might consider installing virtual energy tanks to stabilize the controller, as introduced by Shahriari et al. (2022).

6. CONCLUSION

In this study, we develop a tactile exploration strategy based on unified force-impedance control via local curvature observer to update predefined tactile skill policies by ensuring the tool and contact surface alignment. First, we design a unified force-impedance control that allows the robot to adjust its impedance parameters to the unknown environment. Additionally, the force controller increases the geometry following performance owing to the ensured contact. Second, we use the controller to autonomously observe the local curvature of the environment, designed as a dynamic process. Finally, the tactile exploration performance of the controller is shown by using a polishing skill on the unknown 3D surfaces. As a future work, we will do feature extraction on the saved geometry information in order to further generate motion and force profiles for the new environment.

ACKNOWLEDGEMENTS

We gratefully acknowledge the funding by the European Union's Horizon 2020 research and innovation program as part of the project ReconCycle under grant no. 871352. This work was supported by LongLeif GaPa gGmbH (Geriatronics Project Y). The authors would like to thank the Bavarian State Ministry for Economic Affairs, Regional Development and Energy (StMWi) for supporting the Lighthouse Initiative KI.FABRIK, (Phase 1: Infrastructure as well as the research and development program under, grant no. DIK0249), and the

German Research Foundation (DFG, Deutsche Forschungsgemeinschaft) as part of Germany's Excellence Strategy EXC 2050/1 Project ID 390696704 Cluster of Excellence Centre for Tactile Internet with Human-in-the-Loop (CeTI) of Technische Universität Dresden. The authors acknowledge the financial support by the Federal Ministry of Education and Research of Germany (BMBF) in the programme of "Souverän. Digital. Vernetzt." Joint project 6G-life, project identification number 16KISK002.

Please note that S. Haddadin has a potential conflict of interest as a shareholder of Franka Emika GmbH.

REFERENCES

Balatti, P., Kanoulas, D., Tsagarakis, N., and Ajoudani, A. (2020). A method for autonomous robotic manipulation through exploratory interactions with uncertain environments. *Autonomous Robots*, 44(8), 1395–1410. doi:10.1007/s10514-020-09933-w. URL https://doi.org/10.1007/s10514-020-09933-w.

Ficuciello, F., Villani, L., and Siciliano, B. (2015). Variable impedance control of redundant manipulators for intuitive human–robot physical interaction. *IEEE Transactions on Robotics*, 31(4), 850–863. doi:10.1109/TRO.2015.2430053.

Haddadin, S., Johannsmeier, L., and Díaz Ledezma, F. (2019). Tactile robots as a central embodiment of the tactile internet. In *Proceedings of the IEEE*, volume 107, 471–487.

Haddadin, S., Belder, R., and Albu-Schäffer, A. (2011). Dynamic motion planning for robots in partially unknown environments*. *IFAC Proceedings Volumes*, 44(1), 6842–6850. doi:https://doi.org/10.3182/20110828-6-IT-1002.02500. URL https://www.sciencedirect.com/science/article/pii/S1474667016447051. 18th IFAC World Congress.

Haddadin, S., De Luca, A., and Albu-Schäffer, A. (2017). Robot collisions: A survey on detection, isolation, and identification. *IEEE Transactions on Robotics*, 33(6), 1292–1312. doi:10.1109/TRO.2017.2723903.

Haddadin, S., Parusel, S., Johannsmeier, L., Golz, S., Gabl, S., Walch, F., Sabaghian, M., Jähne, C., Hausperger, L., and Haddadin, S. (2022). The franka emika robot: A reference platform for robotics research and education. *IEEE Robotics Automation Magazine*, 29(2), 46–64. doi:10.1109/MRA.2021.3138382.

Haddadin, S., Urbanek, H., Parusel, S., Burschka, D., Roßmann, J., Albu-Schäffer, A., and Hirzinger, G. (2010). Real-time reactive motion generation based on variable attractor dynamics and shaped velocities. In *2010 IEEE/RSJ International Conference on Intelligent Robots and Systems*, 3109–3116. doi:10.1109/IROS.2010.5650246.

Hamedani, M.H., Sadeghian, H., Zekri, M., Sheikholeslam, F., and Keshmiri, M. (2021). Intelligent Impedance Control using Wavelet Neural Network for dynamic contact force tracking in unknown varying environments. *Control Engineering Practice*, 113, 104840. doi:https://doi.org/10.1016/j.conengprac.2021.104840. URL https://www.sciencedirect.com/science/article/pii/S0967066121001179.

He, W., Chen, Y., and Yin, Z. (2016). Adaptive neural network control of an uncertain robot with full-state constraints. *IEEE Transactions on Cybernetics*, 46(3), 620–629. doi:10.1109/TCYB.2015.2411285.

Hirzinger, G., Albu-Schäffer, A.O., Hähnle, M., Schäfer, I., and Sporer, N. (2001). On a new generation of torque controlled light-weight robots. *Proceedings 2001 ICRA. IEEE International Conference on Robotics and Automation (Cat. No.01CH37164)*, 4, 3356–3363 vol.4.

Hogan, N. (1984). Impedance control: An approach to manipulation. In *1984 American Control Conference*, 304–313. doi:10.23919/ACC.1984.4788393.

Johannsmeier, L., Gerchow, M., and Haddadin, S. (2019). A framework for robot manipulation: Skill formalism, meta learning and adaptive control. *Proceedings - IEEE International Conference on Robotics and Automation*, 2019-May, 5844–5850. doi:10.1109/ICRA.2019.8793542.

Karacan, K., Sadeghian, H., Kirschner, R.J., and Haddadin, S. (2022). Passivity-based skill motion learning in stiffness-adaptive unified force-impedance control. In *2022 IEEE/RSJ International Conference on Intelligent Robots and Systems (IROS)*, in publication. IEEE.

Kato, Y., Balatti, P., Gandarias, J.M., Leonori, M., Tsuji, T., and Ajoudani, A. (2022). A self-tuning impedance-based interaction planner for robotic haptic exploration. *IEEE Robotics and Automation Letters*, 7(4), 9461–9468. doi:10.1109/LRA.2022.3190806.

Khatib, O. (1987). A unified approach for motion and force control of robot manipulators: The operational space formulation. *IEEE J. Robotics Autom.*, 3, 43–53.

Kirschner, R.J., Kurdas, A., Karacan, K., Junge, P., Birjandi, S., Mansfeld, N., Abdolshah, S., and Haddadin, S. (2021). Towards a reference framework for tactile robot performance and safety benchmarking. In *2021 IEEE/RSJ International Conference on Intelligent Robots and Systems (IROS)*, 4290–4297. IEEE.

Kramberger, A., Gams, A., Nemec, B., Schou, C., Chrysostomou, D., Madsen, O., and Ude, A. (2016). Transfer of contact skills to new environmental conditions. In *2016 IEEE-RAS 16th International Conference on Humanoid Robots (Humanoids)*, 668–675. doi:10.1109/HUMANOIDS.2016.7803346.

Kronander, K. and Billard, A. (2016). Stability considerations for variable impedance control. *IEEE Transactions on Robotics*, 32(5), 1298–1305. doi:10.1109/TRO.2016.2593492.

Kulakov, F., Alferov, G.V., Efimova, P., Chernakova, S., and Shymanchuk, D. (2015). Modeling and control of robot manipulators with the constraints at the moving objects. In *2015 International Conference "Stability and Control Processes" in Memory of V.I. Zubov (SCP)*, 102–105. doi:10.1109/SCP.2015.7342075.

Lepora, N.F. and Lloyd, J. (2020). Pose-based servo control with soft tactile sensing. *CoRR*, abs/2012.02504. URL https://arxiv.org/abs/2012.02504.

Ott, C., Dietrich, A., and Albu-Schäffer, A. (2015). Prioritized multi-task compliance control of redundant manipulators. *Automatica*, 53, 416–423. doi:https://doi.org/10.1016/j.automatica.2015.01.015. URL https://www.sciencedirect.com/science/article/pii/S0005109815000163.

Pastor, P., Kalakrishnan, M., Chitta, S., Theodorou, E., and Schaal, S. (2011). Skill learning and task outcome prediction for manipulation. In *2011 IEEE International Conference on Robotics and Automation*, 3828–3834. doi:10.1109/ICRA.2011.5980200.

Pastor, P., Kalakrishnan, M., Righetti, L., and Schaal, S. (2012). Towards associative skill memories. In *2012 12th IEEE-RAS International Conference on Humanoid Robots (Humanoids 2012)*, 309–315. doi:10.1109/HUMANOIDS.2012.6651537.

Qian, Y., Yuan, J., Bao, S., and Gao, L. (2019). Sensorless hybrid normal-force controller with surface prediction. In *2019 IEEE International Conference on Robotics and Biomimetics (ROBIO)*, 83–88. doi:10.1109/ROBIO49542.2019.8961532.

Schindlbeck, C. and Haddadin, S. (2015). Unified Passivity-Based Cartesian Force / Impedance Control for Rigid and Flexible Joint Robots via Task-Energy Tanks. *2015 IEEE International Conference on Robotics and Automation (ICRA)*, 440–447. doi:10.1109/ICRA.2015.7139036.

Shahriari, E., Birjandi, S.A.B., and Haddadin, S. (2022). Passivity-based adaptive force-impedance control for modular multi-manual object manipulation. *IEEE Robotics Autom. Lett.*, 7(2), 2194–2201. doi:10.1109/LRA.2022.3142903. URL https://doi.org/10.1109/LRA.2022.3142903.

Shahriari, E., Kramberger, A., Gams, A., Ude, A., and Haddadin, S. (2017). Adapting to contacts: Energy tanks and task energy for passivity-based dynamic movement primitives. In *2017 IEEE-RAS 17th International Conference on Humanoid Robotics (Humanoids)*, 136–142. IEEE.

Simonič, M., Žlajpah, L., Ude, A., and Nemec, B. (2019). Autonomous learning of assembly tasks from the corresponding disassembly tasks. In *2019 IEEE-RAS 19th International Conference on Humanoid Robots (Humanoids)*, 230–236. doi:10.1109/Humanoids43949.2019.9035052.

Yang, C., Ganesh, G., Haddadin, S., Parusel, S., Albu-Schaeffer, A., and Burdet, E. (2011). Human-like adaptation of force and impedance in stable and unstable interactions. *IEEE transactions on robotics*, 27(5), 918–930.